

Linking Genomic and Physiological Characteristics of Psychrophilic Arthrobacter to Metagenomic Data to Explain Global Environmental Distribution

Liang Shen

Anhui Normal University <https://orcid.org/0000-0003-0374-4198>

Yongqin Liu (✉ yqliu@itpcas.ac.cn)

Institute of Tibetan Plateau Research Chinese Academy of Sciences and CAS Center for Excellence in Tibetan Plateau Earth Sciences <https://orcid.org/0000-0003-2876-7484>

Michelle A. Allen

University of New South Wales - Kensington Campus: University of New South Wales

Baiqing Xu

Institute of Tibetan Plateau Research Chinese Academy of Sciences

Ninglian Wang

Northwest University

Timothy J. Williams

University of New South Wales - Kensington Campus: University of New South Wales

Feng Wang

Institute of Tibetan Plateau Research Chinese Academy of Sciences

Yuguang Zhou

Institute of Microbiology Chinese Academy of Sciences

Qing Liu

Institute of Microbiology Chinese Academy of Sciences

Ricardo Cavicchioli

University of New South Wales - Kensington Campus: University of New South Wales

Research

Keywords: Genomics, metagenomics, psychrophiles, polar environment, alpine environment, microbial adaptation

Posted Date: December 7th, 2020

DOI: <https://doi.org/10.21203/rs.3.rs-119482/v1>

License:  This work is licensed under a Creative Commons Attribution 4.0 International License.

[Read Full License](#)

1 **Linking genomic and physiological characteristics of psychrophilic *Arthrobacter* to**
2 **metagenomic data to explain global environmental distribution**

3

4 **Running title: Polar and alpine *Arthrobacter***

5

6 **Liang Shen^{1,2}, Yongqin Liu^{1,3*}, Michelle A. Allen⁴, Baiqing Xu^{1,3}, Ninglian Wang^{3,5},**
7 **Timothy J. Williams⁴, Feng Wang¹, Yuguang Zhou⁶, Qing Liu⁶, Ricardo Cavicchioli^{4*}**

8

9 ¹Key Laboratory of Tibetan Environment Changes and Land Surface Processes, Institute of
10 Tibetan Plateau Research, Chinese Academy of Sciences, Beijing, 100085, China

11 ²College of Life Sciences, Anhui Normal University, Wuhu, 241000, China

12 ³CAS Center for Excellence in Tibetan Plateau Earth Sciences, Beijing, 100085, China

13 ⁴School of Biotechnology and Biomolecular Sciences, University of New South Wales,
14 Sydney, NSW 2052, Australia

15 ⁵College of Urban and Environmental Science, Northwest University, Xian, 710069, China

16 ⁶China General Microbiological Culture Collection Center (CGMCC), Institute of
17 Microbiology, Chinese Academy of Sciences, Beijing 100101, China

18

19 *Correspondence: yqliu@itpcas.ac.cn

20 ¹Institute of Tibetan Plateau Research, Chinese Academy of Sciences, Beijing, 100101, China

21 r.cavicchioli@unsw.edu.au

22 ⁴School of Biotechnology and Biomolecular Sciences, University of New South Wales,
23 Sydney, NSW 2052, Australia

24 **Abstract**

25 **Background:** Microorganisms drive critical global biogeochemical cycles and dominate the
26 biomass in Earth's expansive cold biosphere. Determining the genomic traits that enable
27 psychrophiles to grow in cold environments informs about their physiology and adaptive
28 responses. However, defining important genomic traits of psychrophiles has proven difficult,
29 with the ability to extrapolate genomic knowledge to environmental relevance proving even
30 more difficult.

31 **Results:** Here we examined the bacterial genus *Arthrobacter*, and assisted by genome
32 sequences of new Tibetan Plateau isolates, defined a clade, Group C, that represents isolates
33 from polar and alpine environments. Group C had a superior ability to grow at -1°C, and
34 possessed genome G+C content, amino acid composition, predicted protein stability and
35 functional capacities (e.g., sulfur metabolism and mycothiol biosynthesis) that distinguished it
36 from non-polar or alpine Group A-*Arthrobacter*. Interrogation of more than 1,000
37 metagenomes identified an over-representation of Group C in Canadian permafrost
38 communities from a simulated spring-thaw experiment, indicative of niche adaptation, and an
39 under-representation of Group A in all polar and alpine samples, indicative of a general
40 response to environmental temperature.

41 **Conclusion:** The findings illustrate a capacity to define genomic markers of specific taxa that
42 potentially have value for environmental monitoring of cold environments, including
43 environmental change arising from anthropogenic impact. More broadly, the study illustrates
44 the challenges involved in extrapolating from genomic and physiological data to an
45 environmental setting.

46

47 **Keywords:** Genomics, metagenomics, psychrophiles, polar environment, alpine environment,
48 microbial adaptation

49

50

51

52 **Background**

53 Many biotic and abiotic factors influence the ability of microorganisms to become indigenous
54 members of environmental communities. Certain environmental factors can limit or prevent
55 the growth of microorganisms, while enhancing, or being essential for others, resulting in
56 ecological niches that support specific microbiome structures [1]. This phenomenon is well
57 illustrated by a Winogradsky column where light and oxygen can be seen to exert major
58 influences on the diversity and the dynamic of microorganisms throughout its length. In more
59 recent times, particularly through technological advancement (e.g., metagenomics), the
60 understanding of microbial ecology and the contributions that microorganisms make to the
61 natural world has grown considerably. Appreciation for microorganisms has accrued from
62 discoveries of new biomes capable of supporting microbial colonization, such as the deep
63 subsurface [2]; new examples of life hidden within microbial ‘dark matter’ (e.g. Asgard
64 archaea [3]), and; the dynamic nature of microbial responses, particularly those that provide
65 surprises, such as the major societal upheaval caused by the COVID19 coronavirus. There is a
66 growing realization that microorganisms constitute the life support system of the biosphere
67 and must be properly accounted for when devising strategies to mitigate the impacts of human
68 activity on the natural world [4]. In essence, we are living in a period in history when the need
69 for society to learn about microbial responses to natural and anthropogenic influences is of
70 unprecedented relevance [4-6].

71 Metagenomic methods have provided a level of insight into microbial communities [7, 8]
72 that could possibly be equated to the advances made by Carl Woese and colleagues when
73 using rRNA sequencing to discover Archaea as the third domain of life. Applied to the cold
74 biosphere, Earth’s single largest biome, metagenomic analyses have catalogued diverse ways
75 in which microbial life has evolved. As an example, Antarctic, marine-derived lake
76 communities have been shown to have evolved independently over their relatively short
77 history of 3,000-5,000 years, adapting not just to low temperature but also to a variety of
78 important environmental factors specific to each lake system (reviewed in REF. [9]).
79 Metagenomic analyses have also begun to be used to uncover the ways in which communities

80 in polar environments respond to changing environmental conditions; for example, the effects
81 of the seasonal polar sunlight cycle on Antarctic marine and marine-derived lake communities
82 [10, 11], and the roles that Arctic bacteria play in melting permafrost acting as a CO₂ source
83 and atmospheric CH₄ sink [12, 13].

84 *Arthrobacter* (Actinobacteria; Micrococcales; Micrococcaceae) are a globally distributed
85 genus of bacteria commonly found in soil, but also in a broad range of environments
86 including water, human skin, and sewage [14-17]. *Arthrobacter* are reported to play important
87 roles in global biogeochemical cycles and decontamination of polluted environments [16, 18].
88 Their responses to temperature, desiccation, ionizing radiation, oxygen radicals, and a range
89 of chemicals have been described [19-21]. Their growth in the laboratory is characterized by
90 nutritional versatility that translates to an ability to grow aerobically in media utilizing a wide
91 range of carbon and nitrogen sources [15]. Some strains closely related to the type species *A.*
92 *globiformis* were isolated from a Lapland glacier region [22], and the identification of
93 psychrophilic species has led to the characterization of a number of *Arthrobacter* enzymes for
94 their biotechnological potential (e.g., REF. [23]). Cold environments that *Arthrobacter* have
95 been isolated from include permafrost and glaciers [24-26].

96 Due to the large scale of the Earth's cold biosphere and its relevance to global
97 biogeochemical cycles, and the biotechnological potential of psychrophiles and their
98 products, numerous studies have been performed to attempt to define the critical traits of
99 psychrophiles (discussed in REFs [9, 23, 27-33]). In the current study, we sequenced the
100 genomes of 13 *Arthrobacter* strains isolated from the Tibetan Plateau and utilized the
101 existence of more than 100 *Arthrobacter* genomes to assess traits that may explain the
102 presence of the genus in naturally cold environments. After identifying a clade characteristic
103 of polar and alpine environments and determining that representatives had a superior ability to
104 grow at low temperature, we used available metagenome data to assess the environmental
105 relevance of the findings. What we learned illustrated the complexities involved in attempting
106 to extrapolate from genomic and physiological data to an environmental setting. It also
107 revealed possible avenues for utilizing *Arthrobacter* as biomarkers of environmental

108 warming.

109

110 **Results**

111 **Phylogenomics**

112 To increase the number of *Arthrobacter* genomes from polar and alpine (PA) environments,
113 isolates from the Tibetan Plateau were sequenced resulting in high-quality genomes (see
114 Materials and methods) for three glacier and 10 lake isolates (Table S1). The phylogenomic
115 relationships of a total of 210 non-redundant high-quality Micrococcaceae genomes were
116 analyzed by constructing ML and Bayesian trees (Fig. S1). The two trees were congruent and
117 most tree-nodes (194/208) were supported by high bootstrap values (>70 %) (Fig. S1). The
118 *Arthrobacter* lineage formed a cluster with 106 representatives that was clearly separated
119 from other Micrococcaceae genera (Fig. S1). The *Arthrobacter* genomes represented PA
120 isolates (total 31, including the 13 new genomes), with the remainder from a broad range of
121 non-polar or alpine (NPA) environments (Table S1).

122 The *Arthrobacter* lineage separated into three clades that branched from the root of the
123 *Arthrobacter* tree (Fig. 1). The 31 PA strains were distributed across the tree, although 11 PA
124 strains formed a cluster with three NPA strains in the central clade (Fig. 1a). Within the
125 central clade, 10 strains grouped together (Fig. 1b, blue font) with an *F* measure of 0.95,
126 defining them as an operationally monophyletic lineage [34]. This was supported by NMDS
127 analysis of amino acid composition (Fig. 1c) and both ANI and AAI distributions (Fig. 1d, e).
128 The grouping of 10 strains (Fig. 1b, blue font) consisted of nine PA strains, plus *A.*
129 *psychrolactophilus* B7 which was isolated from Pennsylvania soil following snow melt; the
130 strain was isolated as a source of cold-active enzymes and was capable of growth at 0 °C [35].
131 The monophyletic lineage of 10 strains was defined as Group C (Fig. 1b, blue font), with all
132 other PA strains as Group B (Fig. 1b, green font), and all strains from NPA environments as
133 Group A (Fig. 1b, red font).

134

135 **Low temperature growth capacity of Group C**

136 To evaluate the growth temperature response of Group A, B and C, three strains from each
137 group were grown at 25, 5 and -1 °C and growth monitored (OD₆₀₀) over time (Fig. 2). The
138 three Group C strains exhibited a markedly enhanced rate of growth at -1 °C (Fig. 2c)
139 particularly compared to Group A strains, and had a reduced rate of growth at 25 °C compared
140 to some of the Group A and B strains (Fig. 2a, b).

141

142 **Genomic characteristics**

143 The size of the 106 *Arthrobacter* genomes ranged from 3.24 – 5.89 Mbp (Table S1). Between
144 Group A and C, no significant differences occurred in genome size, 16S rRNA and tRNA
145 gene copy number, or coding density (Fig. S2). However, a significant difference was
146 observed in amino acid composition and G+C content (Fig. 3, Fig. S2, Table S1). In Group C,
147 the content of N, K, M, I, S, T, F, Q, W and H was significantly higher, while A, E, G, P, D
148 and R was significantly lower (one-way ANOVA, $p < 0.05$, Fig. S3). The correlation between
149 amino acid composition and G+C content was significantly negative for N, I, M, S, F, K, Q
150 and G+C content (R^2 ranged from 0.46 – 0.81; $p < 0.01$), and significantly positive for W, G,
151 D, P, R and A (R^2 ranged from 0.39 – 0.77; $p < 0.01$) (Fig. S4).

152 To evaluate the potential structural relevance of the amino acid compositional
153 differences, temperature-dependent protein stability predictions were made using SCooP,
154 which predicts stability assuming proteins are monomeric and follow a two-state folding
155 transition [36]. From 180 proteins targeted for evaluation (mostly single-copy genes; see
156 Materials and Methods), 86 produced robust stability curves (Fig. 3, Fig. S5, Table S2).
157 Stability was calculated at -1 °C to match the growth temperature at which Group C showed a
158 marked difference in growth ability (Fig. 2). The 86 Group C proteins had significantly higher
159 ΔG values (Group A, -4.27; Group B, -4.29; Group C, -3.60; $p < 0.01$), with 32 proteins being
160 responsible for the reduced predicted stability (Fig. S5, Table S2). These 32 proteins
161 contained a particularly high representation of the amino acids that were most over-
162 represented in Group C (i.e., N, K and R; Fig. S3). The 32 proteins represented 12 functional
163 categories, primarily metabolism (28 proteins; 9 categories), with four involved in respiration,

164 stress response, or cell division and cell cycle (Table S2). The marked amino acid
165 compositional differences, broad representation of functional categories, and high proportion
166 of proteins with predicted decreases in stability ($\sim 1/3^{\text{rd}}$ of those tested), demonstrates that
167 Group C *Arthrobacter* possess broad genomic differences to Group A *Arthrobacter*. If the
168 decreases in predicted protein stability translate to an increased capacity to perform catalysis
169 at low temperature, this may contribute to the higher growth rates of Group C at -1°C (Fig. 2).

170 To further explore the influence of amino acid composition on functional potential, Bray-
171 Curtis distances of genome-wide amino acid composition were evaluated for proteins
172 representing 26 functional categories (Fig. 3). The greatest distance was for the category
173 ‘phages, prophages, transposable elements, plasmids’, consistent with previous studies
174 associating transposable elements with cold adapted microorganisms [37-39]. The functional
175 potential of Group C was also compared to Group A using enrichment analysis [40]
176 performed on proteins representing the 26 functional categories. Group C was over-
177 represented in sulfur metabolism; cofactors, vitamins, prosthetic groups, pigments; protein
178 metabolism; stress response; cell division and cell cycle (Fig. 3, Fig. S6, Table S5), whereas
179 Group A, was over-represented in metabolism of aromatic compounds; nitrogen metabolism;
180 amino acids and derivatives; regulation and cell signaling (Fig. S6, Table S5). The category
181 ‘sulfur metabolism’ also exhibited signatures of amino acid bias (Bray-Curtis distance; Fig.
182 3), suggesting selection for this functional capacity occurred at the levels of both gene
183 complement and amino acid composition.

184 Functional assessments were extended to attempt to identify specific genes unique to
185 Group C. A number of genes involved in the synthesis of amino acids, vitamins, and
186 nucleosides were present in all Group C genomes (Fig. 4). The specific genes also tended to
187 be present in the other four, non-Group C members (Group A and Group B) of the central
188 clade (Fig. 4), but had low representation in other *Arthrobacter* genomes (Fig. 4). The most
189 marked feature was a complete mycothiol (MSH) biosynthesis pathway that was present in all
190 Group C genomes (Fig. 4); MSH is a redox-active thiol, functionally analogous to glutathione
191 (which is typically absent from Actinobacteria), that maintains intracellular redox balance and

192 can therefore protect against oxidative damage [41]. Further, MSH potentially serves as a
193 stable reservoir of carbon and sulfur in bacteria [42]. The ability to respond effectively to
194 oxidative damage may be an important trait of microorganisms from cold environments,
195 particularly for facilitating growth at low temperature limits [43-47]. The MSH pathway was
196 also present in the other four, non-Group C members of the central clade, plus one other
197 Group B member (Fig. 4). Therefore, the MSH pathway plus the individual genes involved in
198 the synthesis of amino acids, vitamins, and nucleosides, are characteristic, but not unique to
199 Group C *Arthrobacter*. If MSH or the other individual genes fulfill roles in facilitating growth
200 at low temperature, the genes may be under stronger positive selection in Group C, while also
201 being retained within Group A and Group B populations (pan genome), but at a significantly
202 lower level.

203 A total of 48 Group C gene families had significantly higher, and 66 had significantly
204 lower average gene copy number compared to Group A, including four which were absent in
205 Group C genomes (Table S6, $p < 0.05$). The absence of two specific genes is noteworthy:
206 adenosylhomocysteinase, which hydrolyzes S-adenosyl-L-homocysteine (a product of methyl
207 transfer reactions that involve S-adenosyl-L-methionine) to homocysteine and adenosine [48];
208 and formate--tetrahydrofolate (THF) ligase, which catalyzes the initial recruitment of single
209 carbon units for THF-mediated one-carbon metabolism [49]. The absence of both genes
210 would be expected to disrupt the synthesis of methionine from homocysteine, and instead
211 favor the alternative pathway of synthesizing methionine from cysteine; the latter pathway
212 may be connected to MSH metabolism, in that accumulation of cysteine (a precursor of MSH
213 synthesis) is toxic to cells [42], so surplus cysteine not required for MSH synthesis, or
214 resulting from MSH degradation, could be directed to methionine synthesis (Table S6).

215 Some of the gene families had particularly high copy numbers per genome (~30 in Group
216 A) with large reductions (~6) in Group C (Table S6); this trend was observed for 3-oxoacyl-
217 [acyl-carrier protein] reductase (FabG), glycerate kinase (GlxK), and alcohol dehydrogenase
218 (Adh). For FabG, this likely reflects a reduced capacity of Group C to catalyze the formation
219 of long-chain fatty acids (Table S6). GlxK is an important catabolic enzyme, in that diverse

220 substrates are degraded to glycerate, and GlxK links these degradation pathways to central
221 carbon metabolism [42]. Decreased copy numbers of Adh likely indicates decreased
222 capacities to utilize alcohols. Thus, decreases in GlxK and Adh might reflect decreased
223 substrate preferences by these *Arthrobacter* strains. It was noteworthy that the copy number
224 of cold shock protein (*csp*) genes was lower in Group C. While *csp* genes are sometimes
225 equated with an ability to grow in the cold or survive cold shock, these nucleic acid binding
226 proteins can perform diverse roles in cellular function (reviewed in REF. [33]); the findings
227 here reinforce the notion that *csp* and other ‘stress’ genes are not good molecular markers for
228 identifying psychrophiles [4, 32].

229

230 **Ecology of Group C *Arthrobacter***

231 We hypothesized that if the laboratory-generated growth data (Fig. 2) and genomic traits (Fig.
232 3) translated to competitiveness in cold environments, Group C *Arthrobacter* would be over-
233 represented in metagenome data from PA vs NPA environments. The relative abundance of
234 *Arthrobacter* in environmental samples (publicly available metagenome data) tends to be low,
235 with no metagenome assembled genomes (MAGs) present in the ~8,000 that were constructed
236 from ~1,500 metagenomes [50], and a total of 12 (> 90% completeness) present in 76,831
237 IMG MAGs (December 2019). To facilitate metagenome analyses, group-specific genes
238 (Table S3) were examined in 797 metagenomes representing PA, temperate and tropical
239 environments (Table S4), with representation shown relative to the *Arthrobacter* pan genome
240 (Fig. 5a) (see **Materials and methods** for description of analytical approach).

241 Group C-specific genes were more highly represented in 11 permafrost metagenomes
242 (Fig. 5b). All of the 11 metagenomes came from a single site: Axel Heiberg Island, Nunavut,
243 Canada [51]. The Axel Heiberg Island study reported 76 metagenomes derived from 1 m
244 cores that were used during a controlled thawing experiment [51]. Most Group C-specific
245 genes were enriched in the 65 cm depth active-layer (7 metagenomes), with one from the 35
246 cm active-layer and three from the 80 cm permafrost-layer (Table S7). A total of 94% of the
247 variability that exists in hits to Group C for the 797 metagenomes (Fig 5b) was traced to pre-

248 existing variability in hits to the *Arthrobacter* pan genome, and when this covariance was
249 removed by ANCOVA analysis, a statistically significant difference in the y-intercepts for the
250 regression lines ($p < 0.0001$) remained; this confirms the over-representation of Group C-
251 specific genes in the 11 metagenomes compared to the remaining 786 metagenomes.

252 To assess whether Group C *Arthrobacter* were generally enriched in permafrost regions,
253 all other publicly available permafrost metagenomes (361 datasets) were analyzed (Fig. 5c). A
254 number appeared somewhat enriched in Group C-specific genes (e.g., a metagenome from
255 Stordalen Mire near Abisko, Sweden; marked by an arrow in Fig. 5c), but as the slopes of the
256 two regression lines were not parallel, it was not valid to compare the y-intercepts, and hence
257 the significance of the difference between them could not be evaluated [52].

258 For Group B-specific genes, no obvious trends separated the PA from NPA metagenomes
259 (Fig. 5d). However, the distribution of Group A-specific genes clustered according to climate,
260 with PA metagenomes showing lower Group A content ($y=0.0161x + 0.1398$, $R^2 = 0.96773$)
261 compared to temperate and tropical metagenomes ($y=0.0244x - 1.8835$, $R^2 = 0.96432$) (Fig.
262 5e). The 11 Axel Heiberg Island metagenomes had a statistically significant under-
263 representation of Group A-specific genes compared to all other metagenomes (ANCOVA, $p <$
264 0.0001). This pattern indicates there is selection against Group A *Arthrobacter* in PA
265 environments, and/or selection for Group A in NPA environments.

266 To attempt to define variables that may explain the niche adaptation of Group C in the
267 Axel Heiberg Island permafrost, available abiotic and biotic data were used from the
268 permafrost study [12, 13]. A range of physicochemical data were available for each of the four
269 depths (5, 35, 65 and 80 cm) but as the timing of sampling for physicochemical data (0, 4, 6,
270 8, 11 and 12 weeks) did not align with the timing of sampling for the metagenomes (0, 0.25,
271 6, 12 and 18 months), the physicochemical data were ultimately not useful for interpreting
272 Group C distribution. Depth, treatment group and sample core did not explain the variation in
273 species composition across the sites, and although incubation time had some explanatory
274 power for the distribution of the entire permafrost study dataset (data not shown), the
275 metagenomes that were enriched in Group C *Arthrobacter* were widely distributed and did

276 not cluster together, suggesting the importance of specific microniches in enrichment of these
277 species. Assessment of functional potential of the microbial communities in each of the 76
278 metagenomes using presence/absence of KO groups also did not identify any significant
279 functional differences (PERMANOVA, $p > 0.05$; data not shown).

280 In contrast, strong taxonomic associations were identified with many members of the
281 microbial community. Analyses were performed to assess taxa that correlated with Group A
282 and Group C, just Group A, and just Group C (Table S8). A total of 107 OTUs positively
283 correlated with Group C *Arthrobacter*, and 63 negatively correlated (Table S8). Of the
284 107 OTUs positively correlated to Group C, 72 were also positively correlated to Group A
285 above the threshold of 0.5 (the remainder were positively correlated with values 0.359 -
286 0.499), and no OTUs were positively correlated to Group A that did not also correlate to
287 Group C. The positively correlating OTUs were dominated by both spore- and non-spore-
288 forming members of Actinobacteria and Firmicutes, as well as members of Proteobacteria; the
289 majority of these OTUs were isolated from soil. Negatively correlating bacterial OTUs
290 mainly belonged to marine or lacustrine members of Bacteroidetes, Cyanobacteria, and
291 Proteobacteria, as well as certain eukaryotes (fungi, plants, marine annelid worm).

292

293 **Discussion**

294 Numerous studies have been performed to attempt to define the critical traits of a
295 psychrophile (discussed in REF. [32, 33, 53]). The current study explored genomic
296 characteristics of a lineage with less than 3.5 % difference in 16S rRNA gene identity. The
297 analyses revealed that the *Arthrobacter* lineage contains a clade with members (Group C)
298 possessing a clear capacity to grow faster than their relatives (Group A and B) under
299 laboratory growth conditions at -1 °C (Fig. 2). Genomic characteristics that potentially
300 explain the physiological capacity include an amino acid composition that is predicted to
301 reduce the stability of a large proportion of proteins thereby enhancing enzyme activity at low
302 temperature [52]. Group C genomes are enriched in sulfur metabolism genes, and sulfur is
303 required for the cysteine component of mycothiol. The synthesis of mycothiol may potentially

304 protect Group C *Arthrobacter* against oxidative damage that may otherwise accumulate as
305 cell division decreases towards the lower temperature limit of growth [43]. Group C also
306 exhibits a relatively high proportion of mobile elements, which is a trait shared with some
307 other cold-adapted microorganisms [37-39]. Collectively, the physiological and genomic traits
308 appear compelling for denoting Group C, a cold-adapted clade of *Arthrobacter*.

309 However, from assessing available metagenome data, we infer that these traits do not
310 translate to a generally enhanced ability to compete in low temperature environments. Other
311 than the 11 specific Axel Heiberg Island permafrost metagenomes, Group C *Arthrobacter*
312 were not highly represented in the other metagenomes from cold environments, including 144
313 from Arctic peat soil, 22 associated with glaciers, 42 from polar deserts, and importantly, 365
314 from other permafrost environments. Even at the Axel Heiberg Island site, Group C-specific
315 genes were not highly abundant at 5 and 20 cm depths. Instead, the pattern of abundance of
316 Group C appears to derive not just from low temperature, but from niche-specific conditions.

317 Attempting to identify specific niche conditions is not trivial. For the Axel Heiberg
318 Island study, the permafrost microbial community was reported to be dominated by
319 Actinobacteria and Proteobacteria, with significant increases at depth for Firmicutes and
320 Actinobacteria and significant decreases for Acidobacteria, Proteobacteria and
321 Verrucomicrobia [13]. However, despite these taxonomic differences, we did not identify
322 significant predicted functional differences by depth. When we turned to specifically
323 correlating the abundance of Group C to OTUs from the metagenome data, a large number of
324 OTUs with positive or negative correlations were identified (Table S8). At a broad level, the
325 environmental data of the positively correlating taxa are consistent with Group C associating
326 with other soil bacteria. While this provides scope for investigating specific taxa that may
327 help shape the niche that Group C occupy, determining which taxa are important and the
328 nature of their interactions will require a dedicated effort.

329 For the negatively correlating cohort, they tend to represent isolates from non-soil
330 environments (Table S8) and may therefore represent non-indigenous microorganisms that
331 have been introduced. The permafrost samples were obtained from an “upland polygonal

332 terrain in proximity to the McGill Arctic Research Station at Expedition Fjord (79°24'57"N,
333 90°45'46"W)" [12]. The prevalence of negatively correlating OTUs matching to
334 Proteobacteria isolated from sea water may reflect aeolian carriage from Expedition Fjord,
335 which is located ~8 km from the Research Station. As the samples were obtained for a
336 simulated permafrost-thaw experiment [51], the negatively correlating OTUs may also reflect
337 environmental disturbance.

338

339 **Conclusions**

340 Our study commenced with the analysis of genome sequences of new Group C *Arthrobacter*
341 isolated from the Tibetan Plateau and progressed through to a rationalization of Group C
342 abundance in global metagenomes. Group C was clearly distinguished from Group A-
343 *Arthrobacter* by possessing genomic signatures consistent with its representation in PA
344 environments and an ability to grow faster when cultivated at -1°C. Assessment of available
345 metagenome data point to the Group C traits as being more relevant to cold niches rather than
346 competitiveness across global permafrost or cold soil environments. The challenge in being
347 able to define the specific niche parameters enabling Group C *Arthrobacter* to be relatively
348 competitive illustrates the inherent difficulties associated with defining 'cause and effect' for
349 explaining 'why' microorganisms reside in the environments in which they are found; that is,
350 the characteristics of the ecological niches that define microbiome structure [1]. Without
351 knowing the specific effectors, the ability to understand and predict responses to
352 environmental changes, is greatly compromised [4, 6, 54, 55]. Establishing long-term data
353 records that include comprehensive metadata associated with monitoring sites, including
354 metadata for each biological sample, will be essential for learning how to link environmental
355 parameters to microbial processes. In a study of sulfate reduction in Arctic marine sediments,
356 growth yield was reasoned to be the most relevant factor for determining competitiveness of
357 sulfate-reducing bacteria in permanently cold marine sediments [53]. These findings illustrate
358 that for cold environments, linking genomic and metagenomic data to measurements of
359 metabolic rates, growth rates and growth yields will undoubtedly help to clarify how specific

360 microbial processes and associated taxa are influenced by environmental temperature.
361 While the characteristics that define the Group C niche are still to be defined, at sites where
362 Group C *Arthrobacter* are relatively abundant they may have value as a biomarker for
363 monitoring the stability of those locations. Moreover, Group A *Arthrobacter* may serve as a
364 more broadly useful biomarker of soil microbial communities. Group A exhibited high
365 relative abundance across NPA metagenomes and relatively low abundance across PA
366 metagenomes. As the data indicate environmental temperature exerts a broad, strong influence
367 on Group A *Arthrobacter*, we predict that environmental warming will generally increase the
368 relative abundance of Group A. Similar influences of environmental temperature have been
369 described for the marine SAR11 clade, including the predicted displacement of polar
370 specialists by phylotypes from warmer latitudes [56]. Depending on how strongly the
371 environmental factors other than temperature select for Group C in permafrost, the apparent
372 broad influence of temperature on Group A suggests it will displace Group C from the niches
373 in which it is currently relatively competitive.

374

375 **Methods**

376 ***Arthrobacter* isolation and genome sequencing**

377 Isolation of *Arthrobacter* strains from glaciers and lakes on the Tibetan Plateau was
378 performed as previously described [25, 26] (Table S1). All strains were deposited in the China
379 General Microbiological Culture Collection Center (CGMCC) with accession numbers:
380 CGMCC 1.16187-1.16198, 1.16223 and 1.16312. Genomic DNA for 16 isolates was
381 extracted using a TIANamp Bacteria DNA Kit (Tiangen, Beijing) following manufacturer's
382 instructions. Paired-end libraries with an insert size of 500 bp were constructed and
383 sequenced using Illumina HiSeq 2000 platform. Prior to *de novo* sequence assembly, low-
384 quality reads were filtered out using Fastp with default options [57]. Filtered sequencing reads
385 were subjected to assembly using SPAdes v3.11.1 with default options [58]. The assembled
386 genome sequences were deposited in DDBJ/ENA/GenBank under the BioProject
387 PRJNA421662.

388

389 **Growth temperature response**

390 *Arthrobacter* strains were grown in R2A broth at 25, 5 and -1°C for up to 10 days with
391 optical density measured at 600 nm (OD_{600}) using a Microplate Reader (MD, SpectraMax
392 M5). For cultivation at -1°C , flasks were placed in ice produced by an ice maker (TKKY,
393 FM40) with flasks placed in a $\sim 4^{\circ}\text{C}$ refrigerator and ice replaced every 12 h. Growth at 5 and
394 25°C was performed using a constant-temperature incubator as described previously [59]. All
395 cultures were grown statically, with flasks swirled to resuspend biomass prior to recording
396 OD_{600} . Strains used for growth temperature profiles were: Group A: *A. luteolus*, *A.*
397 *globiformis* and *A. subterraneus*; Group B: *Arthrobacter* sp. 4R501, *Arthrobacter* sp. 9E14
398 and *Arthrobacter* sp. 08Y14; Group C: *A. alpinus*, *Arthrobacter* sp. A3 and *Arthrobacter* sp.
399 N199823.

400

401 **Preparation of *Arthrobacter* genomes for analysis**

402 As the taxonomic assignment of the genus *Arthrobacter* is not consistent, in August 2018 all
403 genome sequences with the taxonomy identifier 'Arthrobacter' or 'Micrococcaceae' were
404 retrieved from GenBank, providing a total of 427 genomes including the 16 new Tibetan
405 Plateau genomes. The completeness of each genome was calculated using CheckM v1.0.7
406 with default options [60]. Genomes composed of > 300 contigs, with an N50 of < 20 kb,
407 completeness of $< 95\%$, and contamination $> 5\%$ were removed. Genomes were dereplicated
408 to remove genomes with an average amino acid identity (AAI) $\geq 99.5\%$. AAI values were
409 calculated using CompareM with default options (<https://github.com/dparks1134/CompareM>).
410 Average nucleotide identity (ANI) was calculated using the ANI calculator ([http://enve-](http://enve-omics.ce.gatech.edu/ani/)
411 [omics.ce.gatech.edu/ani/](http://enve-omics.ce.gatech.edu/ani/)). A total of 210 genomes met quality requirements, which included
412 13 of the 16 new Tibetan Plateau genomes (Table S1). Gene families were clustered using
413 FastOrtho software (`--pv_cutoff 1-e5 --pi_cutoff 70 --pmatch_cutoff 70`)
414 (<http://enews.patricbrc.org/fastortho/>) with the cutoff values set according to Parks *et al* [34].
415 A gene family matrix was produced using custom PERL scripts, and non-functional based

416 group specific genes were calculated based on this matrix. The annotation of genes was
417 standardized by annotating all genomes using RAST (Rapid Annotation using Subsystem
418 Technology) [61] and PROKKA [62].

419

420 **Phylogenetic and genomic analyses**

421 For phylogenomic clustering, *Cellulomonas carbonis* T26 and *C. fimi* ATCC 484 were chosen
422 as the outgroup as they are close relatives of Micrococcaceae [63], and species that are
423 closely related to the in-group are more suitable for phylogenetic reconstruction than distantly
424 related species [64]. A Maximum Likelihood (ML) phylogenomic tree was constructed using
425 PhyloPhlAn2 with default options [65]. A Bayesian tree was constructed using MPI Mrbayes
426 v3.2 (prset aamodelpr = mixed, mcmc nchains = 16, ngen = 300,000, and leaving other
427 parameter values as default) [66]. The F measure (harmonic mean of precision) provides a
428 metric for determining if taxa are operationally monophyletic (F measure ≥ 0.95) [34]; and
429 was calculated as $F = 2 * ((\text{precision} * \text{recall}) / (\text{precision} + \text{recall}))$. Genome wide amino acid
430 composition was calculated using CompareM with the function aa_usage. The stability curves
431 of proteins were predicted by SCooP [36] using the PDB (Protein Data Bank) files modeled
432 by SWISS-MODEL [67]. The stability equations of the same protein from different hosts
433 were visualized and smoothed using ggplot2 v3.2.1 [68]. The stability curves were analyses
434 for 180 single-copy genes that were shared by most genomes; a small number of genomes had
435 multiple copies of genes, and up to three genomes were permitted to have the absence of the
436 gene in order to account for the use of unclosed genomes (99 of the 106). After retrieval from
437 SWISS-MODEL of all possible PDB files matching the candidate genes, a total of 17,339
438 stability equations were generated (Table S2). Ordination and statistical analyses, including
439 three-dimensional nonmetric multidimensional scaling (3D-NMDS) and gene enrichment
440 analyses were performed with R v3.3.3 and Origin v9.5. For comparisons between Group A,
441 B and C *Arthrobacter*, group-specific genes or functions were defined as being present in
442 95% of the target group (e.g., Group C) genomes and absent in 95% of each of the other
443 group(s) (e.g., Group A) genomes. Group-specific genes were identified (Group A, 74

444 genomes, 16,149 specific genes; Group B, 22 genomes, 4,675 specific genes; Group C, 10
445 genomes, 969 specific genes; Table S3) and normalized to account for the different number of
446 genomes used for each group. To account for differences in gene content between strains,
447 comparisons were calculated relative to the total *Arthrobacter* gene complement from all 106
448 *Arthrobacter* genomes (referred to as the *Arthrobacter* pan genome). Gene copy number was
449 calculated as the average number of the gene for each genome in a group (e.g., Group C),
450 with gene loss or gain calculated from the average copy number for the groups (e.g., Group C
451 vs Group A). To assess the bias of amino acid composition of different functional classes of
452 proteins, genes were assigned to functional categories (assigned by RAST) and total amino
453 acid composition for all proteins from the functional category were compared between groups
454 (e.g., Group C vs Group A). Similarity was measured by Bray-Curtis distance with larger
455 Bray-Curtis distances denoting stronger bias, possibly indicative of selection pressure [40].
456 The functional potential of groups were also compared using enrichment analysis [40].
457 Briefly, the presence or absence of KEGG Ortholog (KO) groups in genomes and
458 metagenomes (see **Collection and analysis of metagenomes**) was assessed [40] and non-
459 parametric one-way ANOVA was used to identify differentially abundant categories using R
460 [69].

461

462 **Collection and analysis of metagenomes**

463 Assembled metagenomes were downloaded from IMG (<https://genome.jgi.doe.gov/portal/>).
464 Classification into polar and alpine (PA) or non-polar or alpine (NPA) environments were
465 made using metadata associated with metagenomes, supplemented by Köppen-Geiger climate
466 classifications (to define temperate and tropical regions) using ArcGIS location data [70].
467 Analyses were initially performed using 797 metagenomes from environments with mean
468 ambient annual temperature (MAT) ranging from -24 °C to 28 °C , representing PA (n = 286,
469 gene count = 244 million), temperate (n = 294, gene count = 291 million), and tropical (n =
470 217, gene count = 981 million) zones (Table S4). Subsequently, all additional (361) available
471 (May 2020) assembled permafrost metagenomes were analyzed. Analyses assessed the

472 relative abundance of each *Arthrobacter* group (A, B and C) using group-specific genes (see
473 **Phylogenetic and genomic analyses**) by performing a local alignment search against the
474 metagenomes using DIAMOND v0.9.24 with the arguments --outfmt 6, --query-cover 70, --id
475 70, --evaluate 1e-5, and leaving others as default [71]. One-way ANCOVA was used to assess
476 statistical differences between regression lines for groups of metagenomes [72] using the data
477 import webform for k=2 at <http://vassarstats.net/vsancova.html>. Correlation analyses were
478 performed between *Arthrobacter* groups and other members of the microbial community from
479 76 metagenomes derived from a simulated permafrost thaw experiment [13]. Operational
480 taxonomic units (OTUs) were assigned from IMG phylodist matches which are based on the
481 top taxon in the IMG isolate database; < 4% of OTUs had < 35% identity. The raw abundance
482 of all OTUs was determined, with 956 meeting the criteria of average abundance ≥ 2 , and
483 detection in at least 56 of the 76 metagenomes. The 956 OTUs were used to construct a
484 correlation matrix using SparCC [73] implemented in python3 with default parameters (20
485 iterations). One hundred simulated datasets were created by random shuffling of the original
486 input with replacement, and their correlation matrices constructed in the same way. The
487 simulated datasets were used to calculate the one- and two-sided pseudo *p*-values. The
488 selected threshold for strong correlations was $> | 0.5 |$. To assess if depth, incubation time,
489 treatment group, sample core, or physicochemical data explained the variation in species
490 composition across permafrost sites, a generalized linear latent variable model was employed
491 as implemented in the R package gllvm [74]. All custom scripts are available at
492 (<https://github.com/environmental-genomes/Arthro>).

493

494 **Acknowledgements**

495 We thank Qilong Qin, Joshua N. Hamm, Pratibha Panwar, Sten Anslan, Saleh Rahimlou, Ping
496 Ren, Fei Liu, Weizhi Song and Wei Zhu for their valuable input related to data analyses, and
497 Maggie Lau, Lyle Whyte and Tullis Onstott for information related to the Axel Heiberg Island
498 site.

499

500 **Authors' contributions**

501 YL, RC, and LS designed the study; YL, BX, and NW collected field samples; YZ and QL
502 provided type strains; LS and FW performed the experiments; LS and MAA analyzed the
503 data; RC, LS, TJW and MAA interpreted the data and wrote the paper.

504

505 **Funding**

506 This study was financially supported by the National Natural Science Foundation of China
507 (Grant Nos. 91851207 and 41701085), the Strategic Priority Research Program of Chinese
508 Academy of Sciences (Grant No. XDA20050101), and the Second Tibetan Plateau Scientific
509 Expedition and Research (STEP) program (Grant No. 2019QZKK0503). The Australian
510 contingent was supported by funding from the Australian Research Council (DP150100244).
511 Liang Shen was funded by the China Scholarship Council (Grant No. 201804910177).

512

513 **Availability of data and materials**

514 The 16 newly isolated *Arthrobacter* strains were deposited in the China General
515 Microbiological Culture Collection Center (CGMCC) with accession numbers: CGMCC
516 1.16187-1.16198, 1.16223 and 1.16312. The assembled genome sequences for newly isolated
517 *Arthrobacter* strains were deposited in DDBJ/ENA/GenBank under the BioProject
518 PRJNA421662. All custom scripts are available at ([https://github.com/environmental-](https://github.com/environmental-genomes/Arthro)
519 [genomes/Arthro](https://github.com/environmental-genomes/Arthro)).

520

521 **Ethics approval and consent to participate**

522 Not applicable.

523

524 **Consent for publication**

525 Not applicable.

526

527 **Competing interests**

528 The authors declare that they have no conflict of interest.

529 **References**

- 530 1. Berg G, Rybakova D, Fischer D, Cernava T, Vergès M-CC, Charles T, et al. Microbiome
531 definition re-visited: old concepts and new challenges. *Microbiome*. 2020;8.
- 532 2. Colman DR, Poudel S, Stamps BW, Boyd ES, Spear JR. The deep, hot biosphere: Twenty-
533 five years of retrospection. *Proc Natl Acad Sci USA*. 2017;114:6895-903.
- 534 3. Zaremba-Niedzwiedzka K, Caceres EF, Saw JH, Backstrom D, Juzokaite L, Vancaester E,
535 et al. Asgard archaea illuminate the origin of eukaryotic cellular complexity. *Nature*.
536 2017;541:353-8.
- 537 4. Cavicchioli R, Ripple WJ, Timmis KN, Azam F, Bakken LR, Baylis M, et al. Scientists'
538 warning to humanity: microorganisms and climate change. *Nat Rev Microbiol*.
539 2019;17:569-86.
- 540 5. Timmis K, Cavicchioli R, Garcia JL, Nogales B, Chavarria M, Stein L, et al. The urgent
541 need for microbiology literacy in society. *Environ Microbiol*. 2019;21:1513-28.
- 542 6. Edwards A, Cameron KA, Cook JM, Debonnaire AR, Furness E, Hay MC, et al. Microbial
543 genomics amidst the Arctic crisis. *Microb Genom*. 2020;6.
- 544 7. Chen LX, Anantharaman K, Shaiber A, Eren AM, Banfield JF. Accurate and complete
545 genomes from metagenomes. *Genome Res*. 2020;30:315-33.
- 546 8. Nkongolo KK, Narendrula-Kotha R. Advances in monitoring soil microbial community
547 dynamic and function. *J Appl Genet*. 2020;61:249-63.
- 548 9. Cavicchioli R. Microbial ecology of Antarctic aquatic systems. *Nat Rev Microbiol*.
549 2015;13:691-706.
- 550 10. Grzymski JJ, Riesenfeld CS, Williams TJ, Dussaq AM, Ducklow H, Erickson M, et al. A
551 metagenomic assessment of winter and summer bacterioplankton from Antarctica
552 Peninsula coastal surface waters. *ISME J*. 2012;6:1901-15.
- 553 11. Panwar P, Allen MA, Williams TJ, Hancock AM, Brazendale S, Bevington J, et al. Influence
554 of the polar light cycle on seasonal dynamics of an Antarctic lake microbial community.
555 *Microbiome*. 2020;8:116.

- 556 12. Lau MCY, Stackhouse BT, Layton AC, Chauhan A, Vishnivetskaya TA, Chourey K, et al.
557 An active atmospheric methane sink in high Arctic mineral cryosols. ISME J. 2015;9:1880-
558 91.
- 559 13. Stackhouse BT, Vishnivetskaya TA, Layton A, Chauhan A, Pfiffner S, Mykytczuk NC, et
560 al. Effects of simulated spring thaw of permafrost from mineral cryosol on CO₂ emissions
561 and atmospheric CH₄ uptake. J Geophys Res Biogeo. 2015;120:1764-84.
- 562 14. Conn H, Dimmick I. Soil bacteria similar in morphology to *Mycobacterium* and
563 *Corynebacterium*. J Bacteriol. 1947;54:291.
- 564 15. Cacciari I, Lippi D. *Arthrobacters*: Successful arid soil bacteria: A review. Arid Soil Res
565 Rehab. 1987;1:1-30.
- 566 16. Niewerth H, Schuldes J, Parschat K, Kiefer P, Vorholt JA, Daniel R, et al. Complete genome
567 sequence and metabolic potential of the quinaldine-degrading bacterium *Arthrobacter* sp.
568 Rue61a. BMC Genomics. 2012;13:534.
- 569 17. Busse HJ, Wieser M. *Arthrobacter*. In: Trujillo ME, Dedysh S, DeVos P, Hedlund B,
570 Kämpfer P, Rainey FA, et al. (eds). Bergey's Manual of Systematics of Archaea and Bacteria.
571 (Wiley, Hoboken, NJ, 2018) pp 1-43.
- 572 18. Unell M, Nordin K, Jernberg C, Stenstrom J, Jansson JK. Degradation of mixtures of
573 phenolic compounds by *Arthrobacter chlorophenolicus* A6. Biodegradation. 2008;19:495-
574 505.
- 575 19. Boylen CW. Survival of *Arthrobacter crystallopoietes* during prolonged periods of extreme
576 desiccation. J Bacteriol. 1973;113:33-7.
- 577 20. Hayashi T, Mukouyama M, Sakano K, Tani Y. Degradation of a sodium acrylate oligomer
578 by an *Arthrobacter* sp. Appl Environ Microbiol. 1993;59:1555-9.
- 579 21. Dsouza M, Taylor MW, Turner SJ, Aislabie J. Genomic and phenotypic insights into the
580 ecology of *Arthrobacter* from Antarctic soils. BMC Genomics. 2015;16:36.
- 581 22. Gounot A. Effects of temperature on the growth of psychrophilic bacteria from glaciers.
582 Can J Microbiol. 1976;22:839-46.
- 583 23. Feller G. Psychrophilic enzymes: from folding to function and biotechnology. Scientifica

- 584 (Cairo). 2013;2013:512840.
- 585 24. Chen X-M, Jiang Y, Li Y-T, Zhang H-H, Li J, Chen X, et al. Regulation of expression of
586 trehalose-6-phosphate synthase during cold shock in *Arthrobacter* strain A3. *Extremophiles*.
587 2011;15:499-508.
- 588 25. Shen L, Liu YQ, Wang N, Jiao NZ, Xu BQ, Liu XB. Variation with depth of the abundance,
589 diversity and pigmentation of culturable bacteria in a deep ice core from the Yuzhufeng
590 Glacier, Tibetan Plateau. *Extremophiles*. 2018;22:29-38.
- 591 26. Liu YQ, Priscu JC, Yao TD, Vick-Majors TJ, Michaud AB, Sheng L. Culturable bacteria
592 isolated from seven high-altitude ice cores on the Tibetan Plateau. *J Glaciol*. 2019;65:29-
593 38.
- 594 27. Margesin R, Feller G. Biotechnological applications of psychrophiles. *Environ Technol*.
595 2010;31:835-44.
- 596 28. Cavicchioli R, Charlton T, Ertan H, Mohd Omar S, Siddiqui KS, Williams TJ.
597 Biotechnological uses of enzymes from psychrophiles. *Microb Biotechnol*. 2011;4:449-60.
- 598 29. Anesio AM, Laybourn-Parry J. Glaciers and ice sheets as a biome. *Trends Ecol Evol*.
599 2012;27:219-25.
- 600 30. Siddiqui KS, Williams TJ, Wilkins D, Yau S, Allen MA, Brown MV, et al. Psychrophiles.
601 *Annu Rev Earth Planet Sci*. 2013;41:87-115.
- 602 31. Boetius A, Anesio MA, Deming WJ, Mikucki AJ, Rapp ZJ. Microbial ecology of the
603 cryosphere: sea ice and glacial habitats. *Nat Rev Microbiol*. 2015;13:677-90.
- 604 32. Cavicchioli R. On the concept of a psychrophile. *ISME J*. 2016;10:793-5.
- 605 33. Collins T, Margesin R. Psychrophilic lifestyles: mechanisms of adaptation and
606 biotechnological tools. *Appl Microbiol Biotechnol*. 2019;103:2857-71.
- 607 34. Parks DH, Chuvochina M, Waite DW, Rinke C, Skarszewski A, Chaumeil PA, et al. A
608 standardized bacterial taxonomy based on genome phylogeny substantially revises the tree
609 of life. *Nat Biotechnol*. 2018;36:996-1004.
- 610 35. Loveland J, Gutshall K, Kasmir J, Prema P, Brenchley JE. Characterization of
611 psychrotrophic microorganisms producing beta-galactosidase activities. *Appl Environ*

- 612 Microbiol. 1994;60:12-8.
- 613 36. Pucci F, Kwasigroch JM, Rooman M. SCooP: an accurate and fast predictor of protein
614 stability curves as a function of temperature. *Bioinformatics*. 2017;33:3415-22.
- 615 37. DeLong EF, Preston CM, Mincer T, Rich V, Hallam SJ, Frigaard N-U, et al. Community
616 genomics among stratified microbial assemblages in the ocean's interior. *Science*.
617 2006;311:496-503.
- 618 38. Lauro FM, Tran K, Vezzi A, Vitulo N, Valle G, Bartlett DH. Large-scale transposon
619 mutagenesis of *Photobacterium profundum* SS9 reveals new genetic loci important for
620 growth at low temperature and high pressure. *J Bacteriol*. 2008;190:1699-709.
- 621 39. Allen MA, Lauro FM, Williams TJ, Burg D, Siddiqui KS, De Francisci D, et al. The genome
622 sequence of the psychrophilic archaeon, *Methanococoides burtonii*: the role of genome
623 evolution in cold adaptation. *ISME J*. 2009;3:1012-35.
- 624 40. Bai Y, Muller DB, Srinivas G, Garrido-Oter R, Potthoff E, Rott M, et al. Functional overlap
625 of the *Arabidopsis* leaf and root microbiota. *Nature*. 2015;528:364-9.
- 626 41. Newton GL, Buchmeier N, Fahey RC. Biosynthesis and functions of mycothiol, the unique
627 protective thiol of Actinobacteria. *Microbiol Mol Biol Rev*. 2008;72:471-94.
- 628 42. Bzimek KP, Newton GL, Ta P, Fahey RC. Mycothiol import by *Mycobacterium smegmatis*
629 and function as a resource for metabolic precursors and energy production. *J Bacteriol*.
630 2007;189:6796-805.
- 631 43. Methé BA, Nelson KE, Deming JW, Momen B, Melamud E, Zhang XJ, et al. The
632 psychrophilic lifestyle as revealed by the genome sequence of *Colwellia psychrerythraea*
633 34H through genomic and proteomic analyses. *Proc Natl Acad Sci USA*. 2005;102:10913-
634 8.
- 635 44. Williams TJ, Lauro FM, Ertan H, Burg DW, Poljak A, Raftery MJ, et al. Defining the
636 response of a microorganism to temperatures that span its complete growth temperature
637 range (-2 °C to 28 °C) using multiplex quantitative proteomics. *Environ Microbiol*.
638 2011;13:2186-203.
- 639 45. Dsouza M, Taylor MW, Turner SJ, Aislabie J. Genome-based comparative analyses of

640 Antarctic and temperate species of *Paenibacillus*. PLoS One. 2014;9:e108009.

641 46. Goordial J, Raymond-Bouchard I, Zolotarov Y, de Bethencourt L, Ronholm J, Shapiro N,
642 et al. Cold adaptive traits revealed by comparative genomic analysis of the
643 eurypsychrophile *Rhodococcus* sp. JG3 isolated from high elevation McMurdo Dry Valley
644 permafrost, Antarctica. FEMS Microbiol Ecol. 2016;92:fiv154.

645 47. Mackelprang R, Burkert A, Haw M, Mahendrarajah T, Conaway CH, Douglas TA, et al.
646 Microbial survival strategies in ancient permafrost: insights from metagenomics. ISME J.
647 2017;11:2305-18.

648 48. Palmer JL, Abeles RH. The mechanism of action of S-adenosylhomocysteinase. J Biol
649 Chem. 1979;254:1217-26.

650 49. Sah S, Aluri S, Rex K, Varshney U. One-carbon metabolic pathway rewiring in *Escherichia*
651 *coli* reveals an evolutionary advantage of 10-formyltetrahydrofolate synthetase (Fhs) in
652 survival under hypoxia. J Bacteriol. 2015;197:717-26.

653 50. Parks DH, Rinke C, Chuvochina M, Chaumeil PA, Woodcroft BJ, Evans PN, et al. Recovery
654 of nearly 8,000 metagenome-assembled genomes substantially expands the tree of life. Nat
655 Microbiol. 2017;2:1533-42.

656 51. Chauhan A, Layton AC, Vishnivetskaya TA, Williams D, Pfiffner SM, Rekepalli B, et al.
657 Metagenomes from thawing low-soil-organic-carbon mineral cryosols and permafrost of
658 the canadian high arctic. Genome Announc. 2014;2:e01217-14.

659 52. Siddiqui KS, Cavicchioli R. Cold-adapted enzymes. Annu Rev Biochem. 2006;75:403-33.

660 53. Scholze C, Jørgensen BB, Røy H. Psychrophilic properties of sulfate-reducing bacteria in
661 Arctic marine sediments. Limnol Oceanogr. 2020:10.1002/lno.11586.

662 54. Webster NS, Wagner M, Negri AP. Microbial conservation in the Anthropocene. Environ
663 Microbiol. 2018;20:1925-8.

664 55. Cavicchioli R. A vision for a 'microbcentric' future. Microb Biotechnol. 2019;12:26-9.

665 56. Brown MV, Lauro FM, DeMaere MZ, Muir L, Wilkins D, Thomas T, et al. Global
666 biogeography of SAR11 marine bacteria. Mol Syst Biol. 2012;8:595.

667 57. Chen S, Zhou Y, Chen Y, Gu J. fastp: an ultra-fast all-in-one FASTQ preprocessor.

668 Bioinformatics. 2018;34:i884-90.

669 58. Bankevich A, Nurk S, Antipov D, Gurevich AA, Dvorkin M, Kulikov AS, et al. Spades: A
670 new genome assembly algorithm and its applications to single-cell sequencing. *J Comput*
671 *Biol.* 2012;19:455-77.

672 59. Shen L, Liu YQ, Xu BQ, Wang NL, Zhao HB, Liu XB, et al. Comparative genomic analysis
673 reveals the environmental impacts on two *Arcticibacter* strains including sixteen
674 Sphingobacteriaceae species. *Sci Rep.* 2017;7:2055.

675 60. Parks DH, Imelfort M, Skennerton CT, Hugenholtz P, Tyson GW. CheckM: assessing the
676 quality of microbial genomes recovered from isolates, single cells, and metagenomes.
677 *Genome Res.* 2015;25:1043.

678 61. Overbeek R, Olson R, Pusch GD, Olsen GJ, Davis JJ, Disz T, et al. The SEED and the rapid
679 annotation of microbial genomes using subsystems technology (RAST). *Nucleic Acids Res.*
680 2014;42:D206-14.

681 62. Seemann T. Prokka: rapid prokaryotic genome annotation. *Bioinformatics.* 2014;30:2068-
682 9.

683 63. Yarza P, Richter M, Peplies J, Euzéby J, Amann R, Schleifer KH, et al. The All-Species
684 Living Tree project: A 16S rRNA-based phylogenetic tree of all sequenced type strains.
685 *Syst Appl Microbiol.* 2008;31:241-50.

686 64. Yang ZH. Computational molecular evolution. Great Britain: Oxford University Press;
687 2006.

688 65. Segata N, Bornigen D, Morgan XC, Huttenhower C. PhyloPhlAn is a new method for
689 improved phylogenetic and taxonomic placement of microbes. *Nat Commun.* 2013;4:2304.

690 66. Ronquist F, Teslenko M, van der Mark P, Ayres DL, Darling A, Hohna S, et al. MrBayes
691 3.2: efficient Bayesian phylogenetic inference and model choice across a large model space.
692 *Syst Biol.* 2012;61:539-42.

693 67. Schwede T, Kopp J, Guex N, Peitsch MC. SWISS-MODEL: An automated protein
694 homology-modeling server. *Nucleic Acids Res.* 2003;31:3381-5.

695 68. Wickham H. ggplot2: Elegant graphics for data analysis. New York: Springer; 2016.

- 696 69. Ihaka R, Gentleman R. R: A language for data analysis and graphics. *J Comput Graph Statist.*
697 1996;5:299-314.
- 698 70. Peel MC, Finlayson BL, McMahon TA. Updated world map of the Köppen-Geiger climate
699 classification. *Hydrol Earth Syst Sci.* 2007;11:259-63.
- 700 71. Buchfink B, Xie C, Huson DH. Fast and sensitive protein alignment using DIAMOND. *Nat*
701 *Methods.* 2015;12:59-60.
- 702 72. McDonald JH. *Handbook of Biological Statistics* (3rd ed.). Baltimore, Maryland: Sparky
703 House Publishing; 2014.
- 704 73. Friedman J, Alm EJ. Inferring correlation networks from genomic survey data. *PLoS*
705 *Comput Biol.* 2012;8:e1002687.
- 706 74. Niku J, Hui FKC, Taskinen S, Warton DI. gllvm: Fast analysis of multivariate abundance
707 data with generalized linear latent variable models in R. *Methods Ecol Evol.* 2019;10:2173–
708 82.

709
710

711 **Fig. 1 *Arthrobacter* phylogeny and genome compositional profiling.** (a) Maximum
712 Likelihood *Arthrobacter* phylogenomic tree. The *Arthrobacter* portion of ML Micrococcaceae
713 phylogenomic tree (Fig. S1a) is reproduced with each leaf marked as polar and alpine (PA,
714 grey highlight) or non-polar and alpine (NPA). The tree has three major clades with the
715 central clade highlighted (purple box). (b) As for (a) except strain names denoted and font
716 color used to depict Group A (red font; NPA environments), Group B (green font; PA
717 environments clustering with sequences from NPA environments) and Group C (blue font; PA
718 environments that formed an operationally monophyletic lineage with an *F* measure of 0.95).
719 The specific types of cold environments from where Group C *Arthrobacter* were isolated are
720 shown to the right of tree. (c) 3D-NMDS plot of genome-wide amino acid composition. (d)
721 Distribution of pairwise ANI. (e) Distribution of pairwise AAI.

722

723 **Fig. 2 Growth temperature profiles of Group A, B and C *Arthrobacter*.** OD₆₀₀ growth

724 curves for representative *Arthrobacter* of Group A (red symbols and line; *A. luteolus*, *A.*
725 *globiformis* and *A. subterraneus*), Group B (green symbols and line; *Arthrobacter* sp. 4R501,
726 *Arthrobacter* sp. 9E14 and *Arthrobacter* sp. 08Y14) and Group C (blue symbols and line; *A.*
727 *alpinus*, *Arthrobacter* sp. A3 and *Arthrobacter* sp. N199823) at (a) 25 °C, (b) 5 °C and (c) -
728 1 °C.

729

730 **Fig. 3 Overview of genomic characteristics of Group C *Arthrobacter*.** (a) Box plot of G+C
731 content. Group A (red); Group C (blue); boxes represent the interquartile range with
732 horizontal lines showing maximum and minimum values, excluding outliers. Group C had
733 significantly lower G+C content. (b) Scatter plot of amino acid composition. Group A (light
734 red circles); Group C (blue circles); ***, $P < 0.005$; *, $P = 0.05 - 0.01$; ns, not significant.
735 The composition of numerous amino acids varied significantly between Group C and Group A
736 *Arthrobacter*. (c) Protein stability predictions calculated using SCooP. Group A (red line);
737 Group C (blue line). The curve is for coenzyme A biosynthesis bifunctional protein, CoaC,
738 and is representative of one of the 32 Group C proteins from a total of 86 which had reduced
739 predicted stability (Table S2, Fig. S5) (d) Box plot of amino acid bias for functional
740 categories. Boxes represent the interquartile range of the Bray-Cruze distances; lines
741 extending from boxes show the maximum and minimum Bray-Cruze distances; dots beyond
742 the lines represent outliers. Biases in amino acid composition (b) were reflected in specific
743 functional categories. (e) Representation of functional categories. Specific functional
744 categories were over- or under-represented in Group C; arrows indicate relative increases (up
745 arrow) or decreases (down arrow) in functional categories in Group C. (f) Representation of
746 specific functions. Specific functional processes defined by genes or pathways were
747 characteristic of Group C (up arrow) or had a restricted capacity in Group C (down arrow)
748 compared to Group A (also see Fig. 4).

749

750 **Fig. 4 *Arthrobacter* genes typifying the functional potential of Group C.** (a) ML
751 *Arthrobacter* phylogenomic tree as for Fig. 1. (b) Heat map of the representation of specific

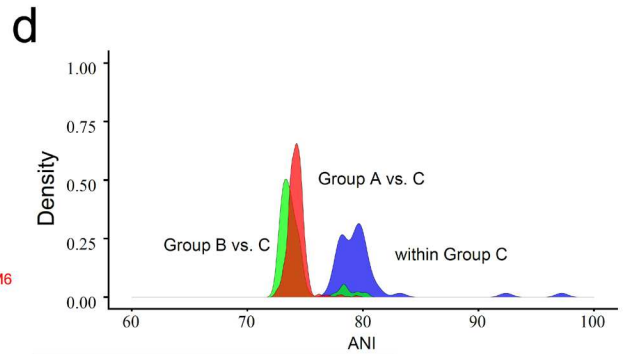
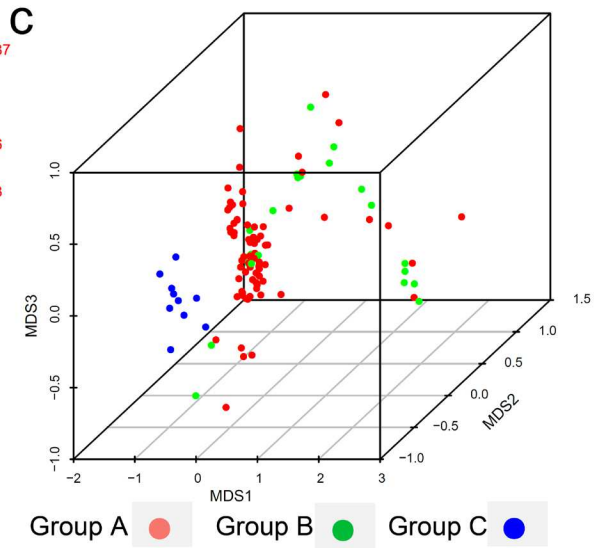
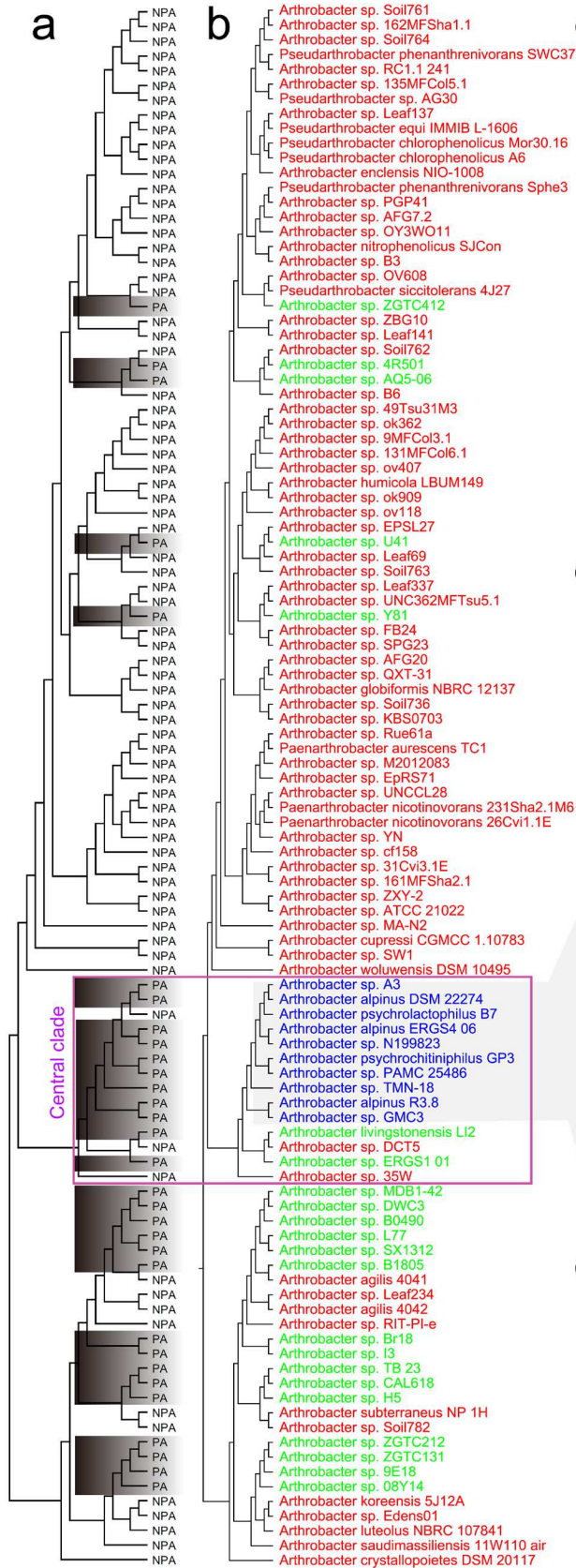
752 genes in *Arthrobacter* genomes, highlighting those present in Group C and the central clade. *i*,
753 branched-chain acyl-CoA dehydrogenase; *ii*, enoyl-CoA hydratase; *iii*, biotin repressor; *iv*,
754 hydrolase in cluster with formaldehyde/S-nitrosomethylol reductase; *v*, methylol-dependent
755 formaldehyde dehydrogenase.

756

757 **Fig. 5 Metagenome analysis of Group C *Arthrobacter*.** (a) Depiction of the (mean annual
758 temperature (MAT) of surface air at a height of 2 m ([European Centre for Medium-Range](#)
759 [Weather Forecasts](#)) relative to latitude. The 797 metagenomes are divided into thermal
760 categories: PA (black squares, 286 metagenome), temperate (grey squares, 294 metagenomes)
761 and tropical (purple squares, 217 metagenomes). (b) Linear regression showing the
762 correlation of the abundance of Group C-specific genes within each of the 797 metagenomes
763 (see panel (a)) relative to the abundance of Group C-specific genes within the *Arthrobacter*
764 pan genome. The 95% prediction interval (dark red band) and 95% confidence interval (light
765 red band) is shown for each regression line (panels b, c and e). The upper cluster contains 11
766 Axel Heiberg Island permafrost metagenomes. (c) As for panel (b), except with the addition
767 of 361 permafrost metagenomes (total 1158 metagenomes). The Stordalen Mire (Abisko,
768 Sweden) metagenome is shown by an arrow. (d) As for panel (b), except showing Group B-
769 specific genes. (e) As for panel (b), except showing Group A-specific genes present in PA
770 genomes (lower line) and NPA genomes (upper line). The regression line for the 11 Axel
771 Heiberg Island permafrost metagenomes is not shown.

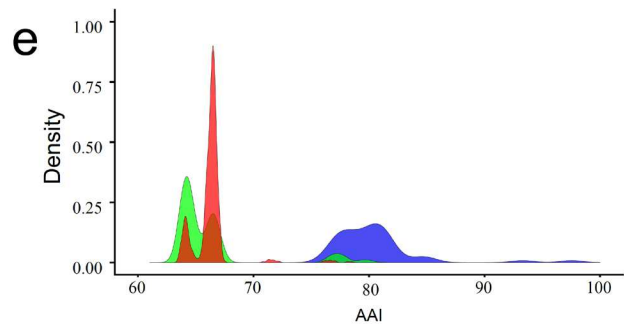
772

773

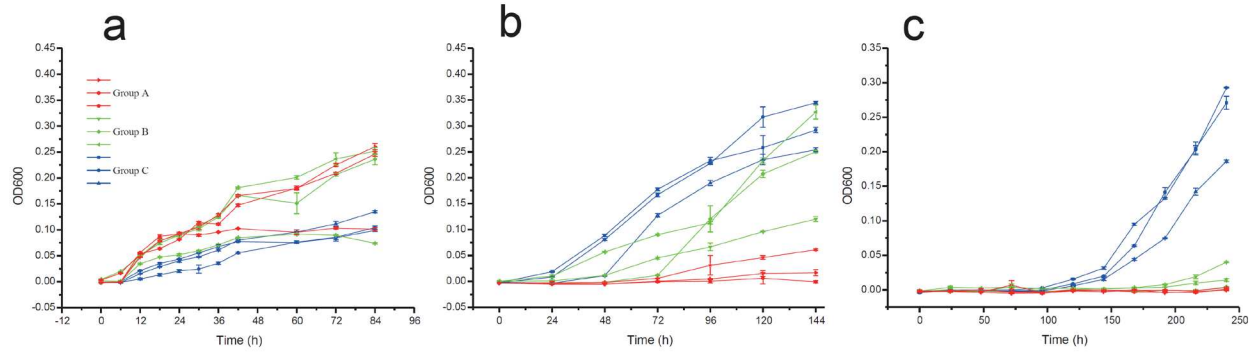


Tibetan Plateau, permafrost
 Alps, soil
 Pennsylvania, soil
 Tibetan Plateau, glacier
 Tibetan Plateau, glacier
 Antarctica, soil
 Arctic, soil
 Tibetan Plateau, glacier
 Antarctica, soil
 Tibetan Plateau, lake

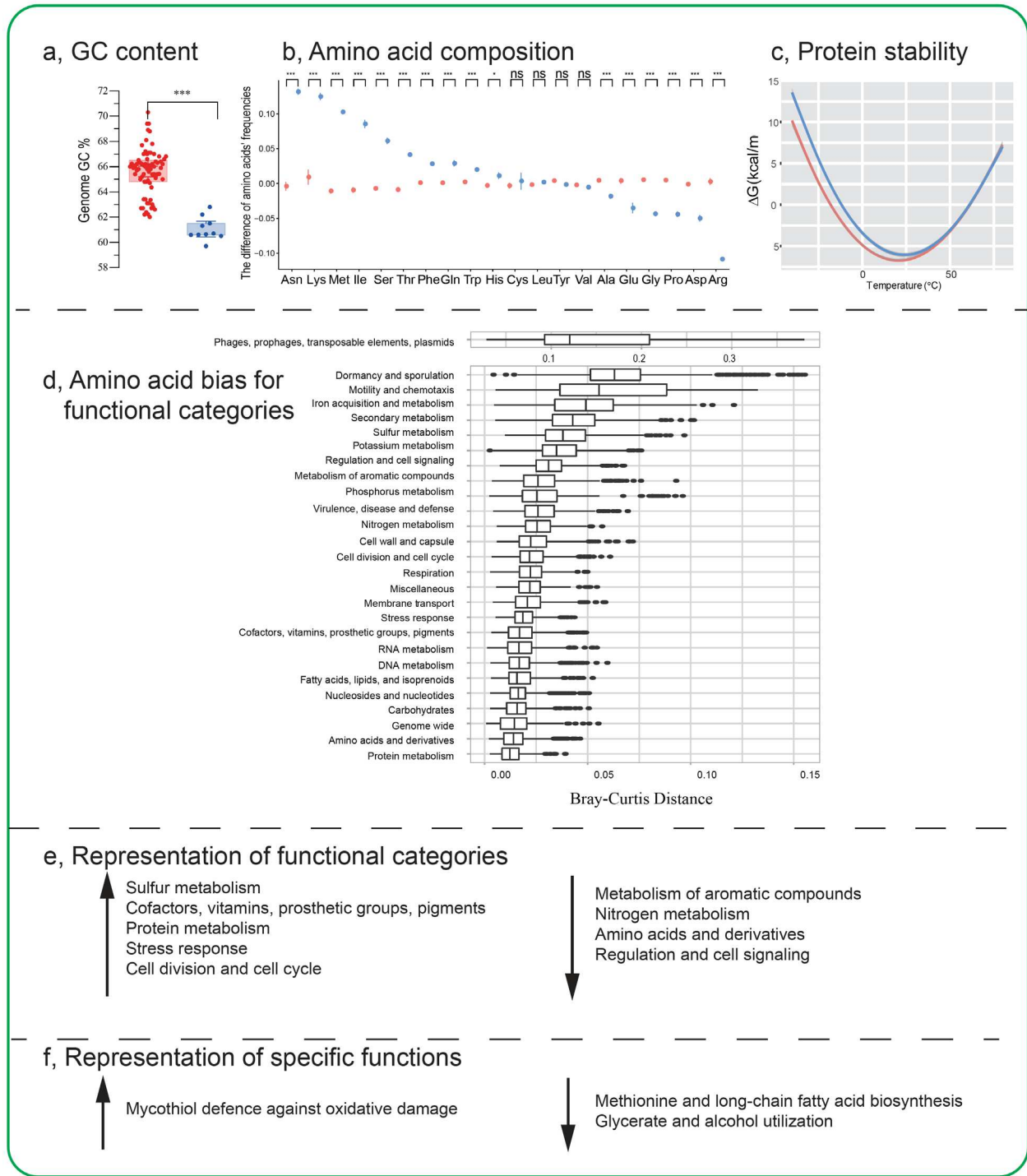
Group C



2 **Fig. 1 *Arthrobacter* phylogeny and genome compositional profiling.** (a) Maximum Likelihood
3 *Arthrobacter* phylogenomic tree. The *Arthrobacter* portion of ML Micrococcaceae phylogenomic tree
4 (Fig. S1a) is reproduced with each leaf marked as polar and alpine (PA, grey highlight) or non-polar and
5 alpine (NPA). The tree has three major clades with the central clade highlighted (purple box). (b) As for
6 (a) except strain names denoted and font color used to depict Group A (red font; NPA environments),
7 Group B (green font; PA environments clustering with sequences from NPA environments) and Group C
8 (blue font; PA environments that formed an operationally monophyletic lineage with an *F* measure of
9 0.95). The specific types of cold environments from where Group C *Arthrobacter* were isolated are shown
10 to the right of tree. (c) 3D-NMDS plot of genome-wide amino acid composition. (d) Distribution of
11 pairwise ANI. (e) Distribution of pairwise AAI.



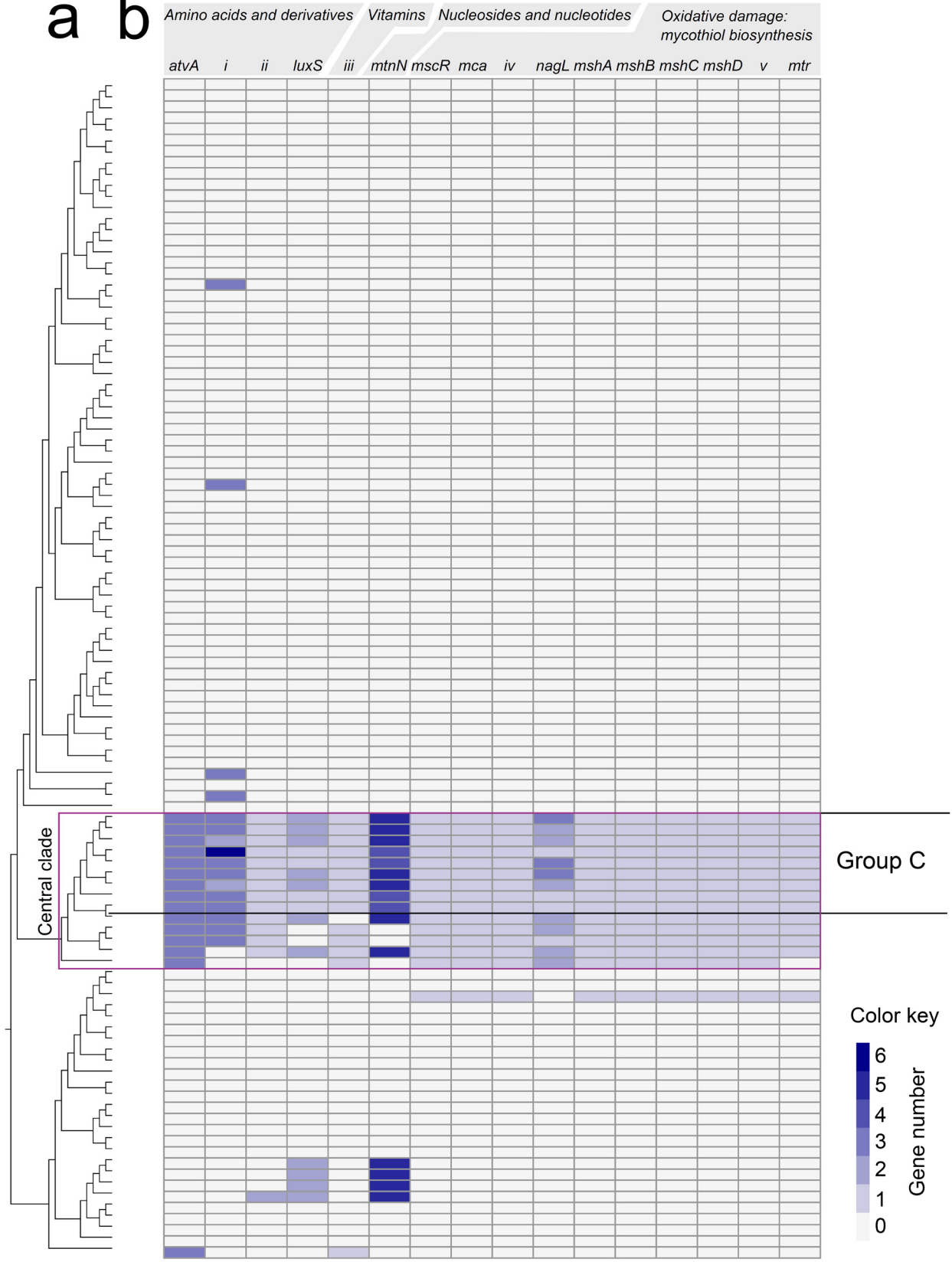
1
 2
 3 **Fig. 2 Growth temperature profiles of Group A, B and C *Arthrobacter*.** OD₆₀₀ growth curves for
 4 representative *Arthrobacter* of Group A (red symbols and line; *A. luteolus*, *A. globiformis* and *A.*
 5 *subterraneus*), Group B (green symbols and line; *Arthrobacter* sp. 4R501, *Arthrobacter* sp. 9E14 and
 6 *Arthrobacter* sp. 08Y14) and Group C (blue symbols and line; *A. alpinus*, *Arthrobacter* sp. A3 and
 7 *Arthrobacter* sp. N199823) at (a) 25 °C, (b) 5 °C and (c) -1 °C.



1
2
3 **Fig. 3 Overview of genomic characteristics of Group C *Arthrobacter*.** (a) Box plot of G+C content.
4 Group A (red); Group C (blue); boxes represent the interquartile range with horizontal lines showing
5 maximum and minimum values, excluding outliers. Group C had significantly lower G+C content. (b)
6 Scatter plot of amino acid composition. Group A (light red circles); Group C (blue circles); ***, $P <$
7 0.005; *, $P = 0.05 - 0.01$; ns, not significant. The composition of numerous amino acids varied
8 significantly between Group C and Group A *Arthrobacter*. (c) Protein stability predictions calculated using

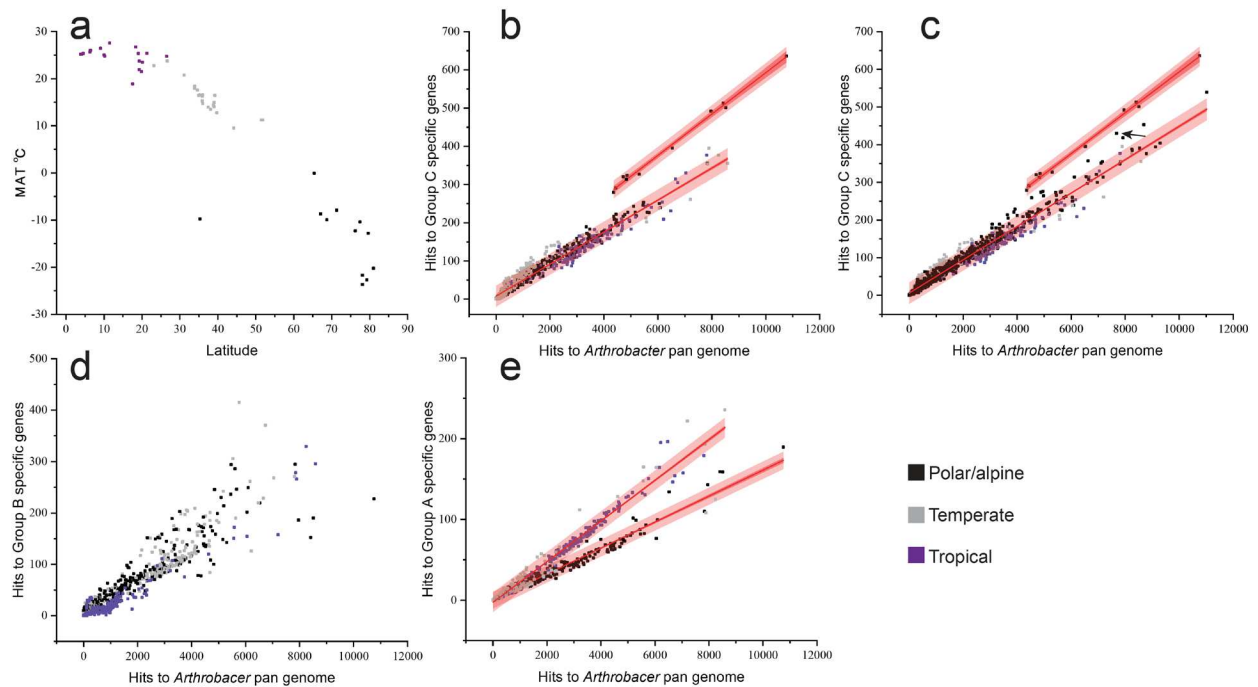
9 SCooP. Group A (red line); Group C (blue line). The curve is for coenzyme A biosynthesis bifunctional
10 protein, CoaC, and is representative of one of the 32 Group C proteins from a total of 86 which had
11 reduced predicted stability (Table S2, Fig. S5) **(d)** Box plot of amino acid bias for functional categories.
12 Boxes represent the interquartile range of the Bray-Cruze distances; lines extending from boxes show the
13 maximum and minimum Bray-Cruze distances; dots beyond the lines represent outliers. Biases in amino
14 acid composition (b) were reflected in specific functional categories. **(e)** Representation of functional
15 categories. Specific functional categories were over- or under-represented in Group C; arrows indicate
16 relative increases (up arrow) or decreases (down arrow) in functional categories in Group C. **(f)**
17 Representation of specific functions. Specific functional processes defined by genes or pathways were
18 characteristic of Group C (up arrow) or had a restricted capacity in Group C (down arrow) compared to
19 Group A (also see Fig. 4).

a b



1
2

3 **Fig. 4 *Arthrobacter* genes typifying the functional potential of Group C. (a)** ML *Arthrobacter*
4 phylogenomic tree as for Fig. 1. **(b)** Heat map of the representation of specific genes in *Arthrobacter*
5 genomes, highlighting those present in Group C and the central clade. *i*, branched-chain acyl-CoA
6 dehydrogenase; *ii*, enoyl-CoA hydratase; *iii*, biotin repressor; *iv*, hydrolase in cluster with formaldehyde/S-
7 nitrosomycothiols reductase; *v*, mycothiol-dependent formaldehyde dehydrogenase.



1
2
3 **Fig. 5 Metagenome analysis of Group C *Arthrobacter*.** (a) Depiction of the (mean annual temperature
4 (MAT) of surface air at a height of 2 m ([European Centre for Medium-Range Weather Forecasts](#)) relative
5 to latitude. The 797 metagenomes are divided into thermal categories: PA (black squares, 286
6 metagenome), temperate (grey squares, 294 metagenomes) and tropical (purple squares, 217
7 metagenomes). (b) Linear regression showing the correlation of the abundance of Group C-specific genes
8 within each of the 797 metagenomes (see panel (a)) relative to the abundance of Group C-specific genes
9 within the *Arthrobacter* pan genome. The 95% prediction interval (dark red band) and 95% confidence
10 interval (light red band) is shown for each regression line (panels b, c and e). The upper cluster contains 11
11 Axel Heiberg Island permafrost metagenomes. (c) As for panel (b), except with the addition of 361
12 permafrost metagenomes (total 1158 metagenomes). The Stordalen Mire (Abisko, Sweden) metagenome
13 is shown by an arrow. (d) As for panel (b), except showing Group B-specific genes. (e) As for panel (b),
14 except showing Group A-specific genes present in PA genomes (lower line) and NPA genomes (upper
15 line). The regression line for the 11 Axel Heiberg Island permafrost metagenomes is not shown.

Figures

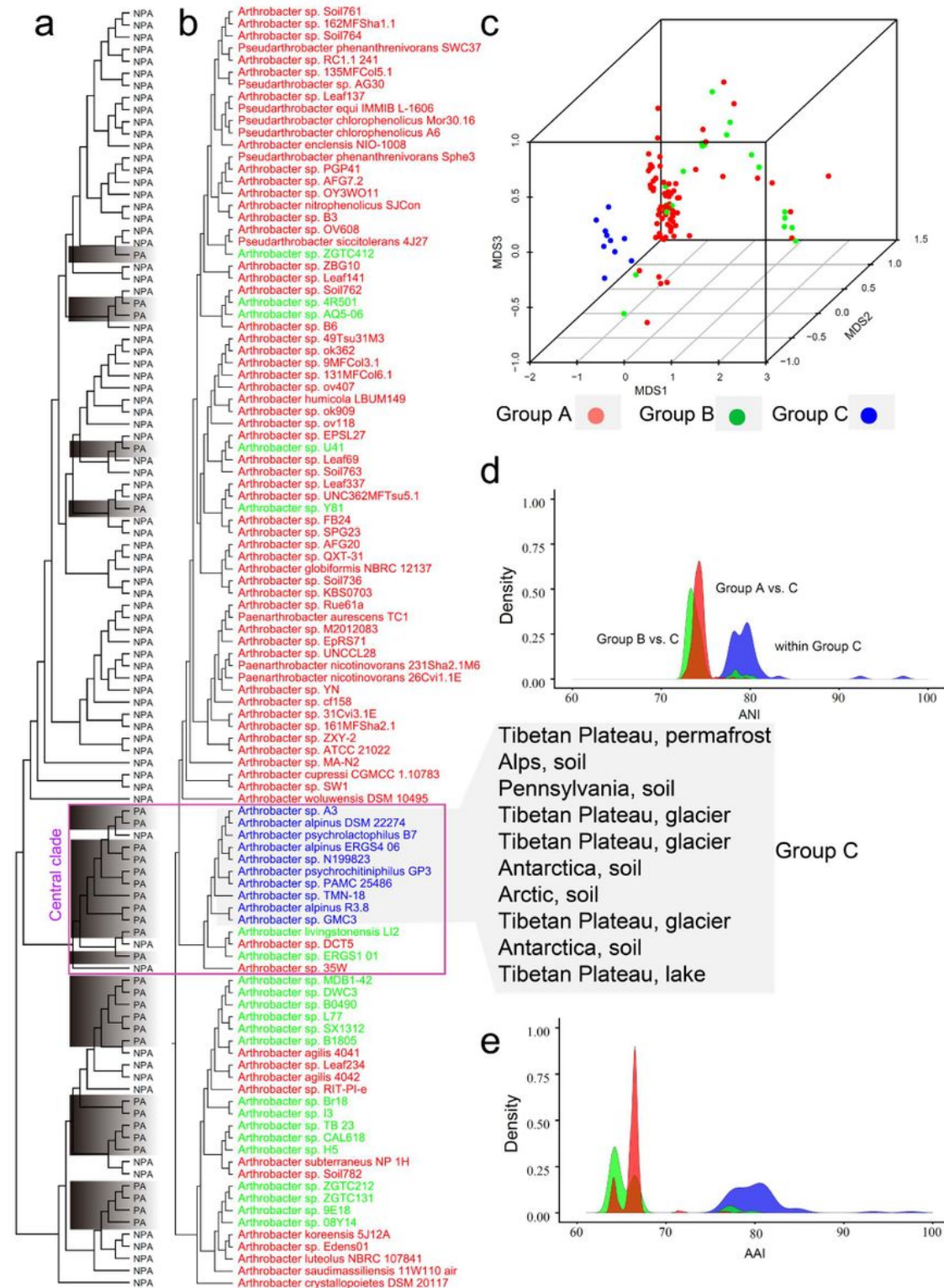


Figure 1

Arthrobacter phylogeny and genome compositional profiling. (a) Maximum Likelihood Arthrobacter phylogenomic tree. The Arthrobacter portion of ML Micrococcaceae phylogenomic tree (Fig. S1a) is reproduced with each leaf marked as polar and alpine (PA, grey highlight) or non-polar and alpine (NPA).

The tree has three major clades with the central clade highlighted (purple box). (b) As for (a) except strain names denoted and font color used to depict Group A (red font; NPA environments), Group B (green font; PA environments clustering with sequences from NPA environments) and Group C (blue font; PA environments that formed an operationally monophyletic lineage with an F measure of 0.95). The specific types of cold environments from where Group C *Arthrobacter* were isolated are shown to the right of tree. (c) 3D-NMDS plot of genome-wide amino acid composition. (d) Distribution of pairwise ANI. (e) Distribution of pairwise AAI.

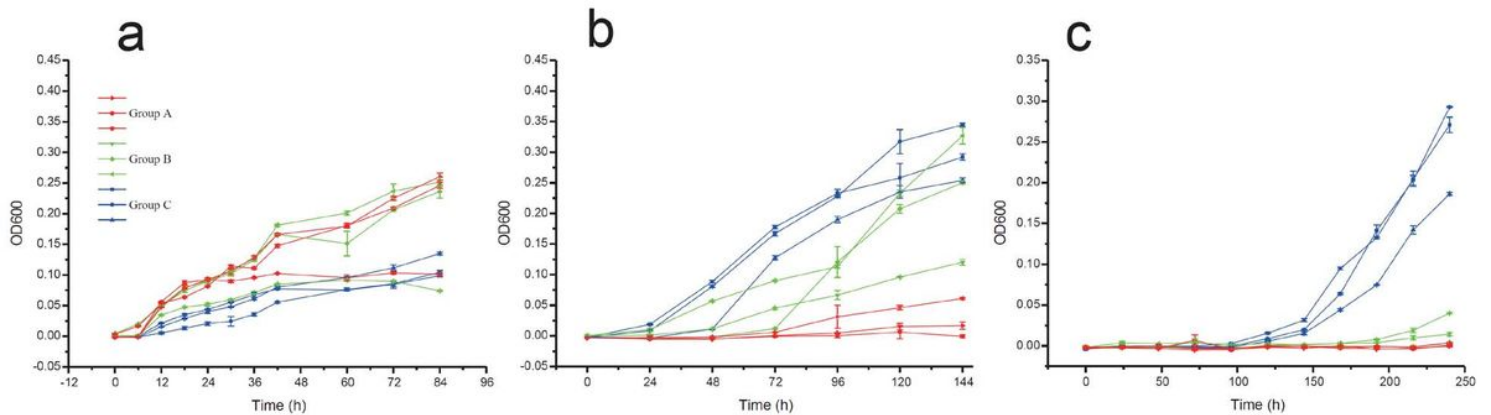


Figure 2

Growth temperature profiles of Group A, B and C *Arthrobacter*. OD600 growth curves for representative *Arthrobacter* of Group A (red symbols and line; *A. luteolus*, *A. globiformis* and *A. subterraneus*), Group B (green symbols and line; *Arthrobacter* sp. 4R501, *Arthrobacter* sp. 9E14 and *Arthrobacter* sp. 08Y14) and Group C (blue symbols and line; *A. alpinus*, *Arthrobacter* sp. A3 and *Arthrobacter* sp. N199823) at (a) 25 °C, (b) 5 °C and (c) -1 °C.

and Group A *Arthrobacter*. (c) Protein stability predictions calculated using SCooP. Group A (red line); Group C (blue line). The curve is for coenzyme A biosynthesis bifunctional protein, CoaC, and is representative of one of the 32 Group C proteins from a total of 86 which had reduced predicted stability (Table S2, Fig. S5) (d) Box plot of amino acid bias for functional categories. Boxes represent the interquartile range of the Bray-Cruze distances; lines extending from boxes show the maximum and minimum Bray-Cruze distances; dots beyond the lines represent outliers. Biases in amino acid composition (b) were reflected in specific functional categories. (e) Representation of functional categories. Specific functional categories were over- or under-represented in Group C; arrows indicate relative increases (up arrow) or decreases (down arrow) in functional categories in Group C. (f) Representation of specific functions. Specific functional processes defined by genes or pathways were characteristic of Group C (up arrow) or had a restricted capacity in Group C (down arrow) compared to Group A (also see Fig. 4).

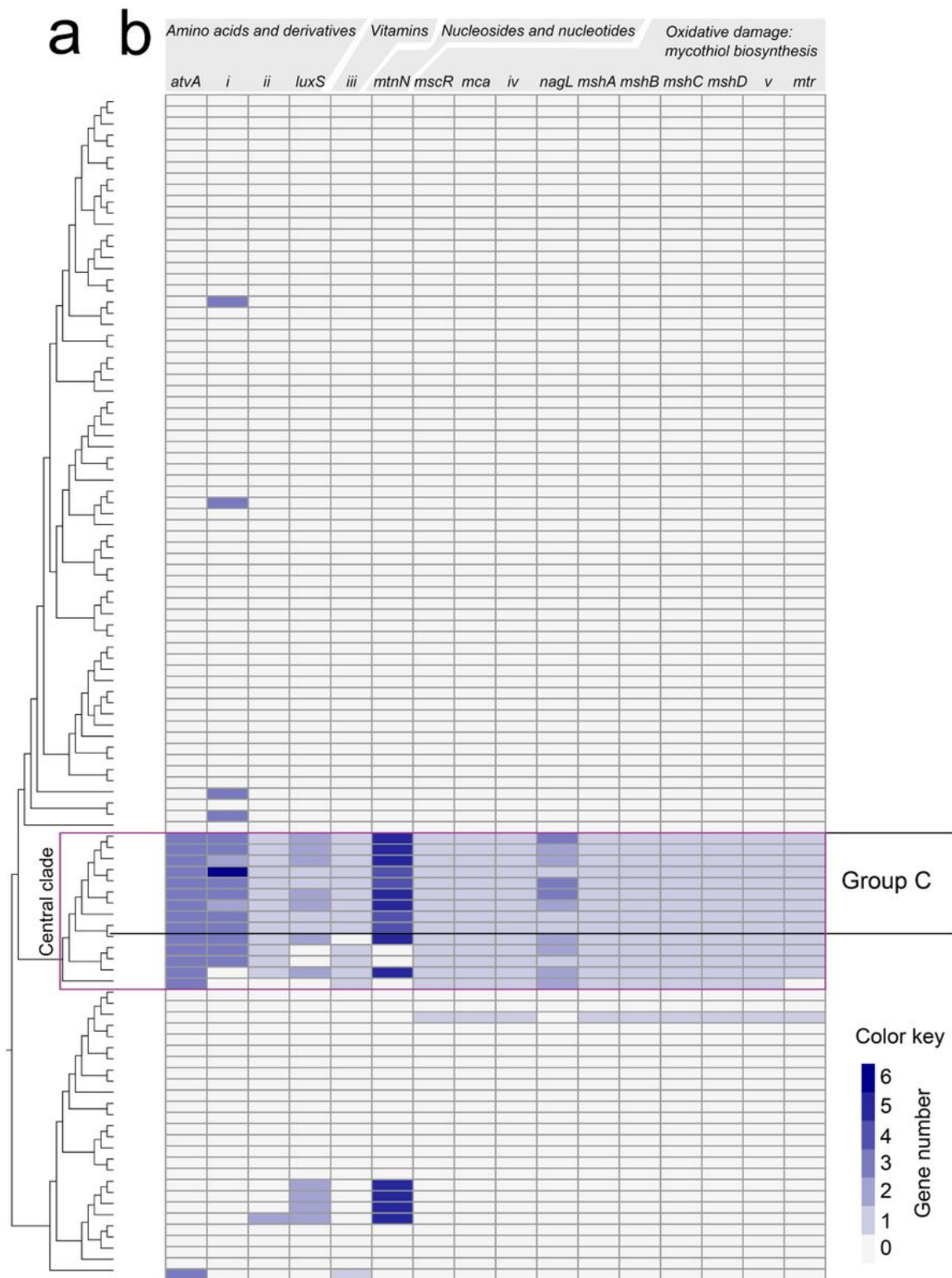


Figure 4

Arthrobacter genes typifying the functional potential of Group C. (a) ML Arthrobacter phylogenomic tree as for Fig. 1. (b) Heat map of the representation of specific genes in Arthrobacter genomes, highlighting those present in Group C and the central clade. \square , branched-chain acyl-CoA dehydrogenase; \square , enoyl-CoA hydratase; \square , biotin repressor; \square , hydrolase in cluster with formaldehyde/S nitrosomycothiol reductase; \square , mycothiol-dependent formaldehyde dehydrogenase.

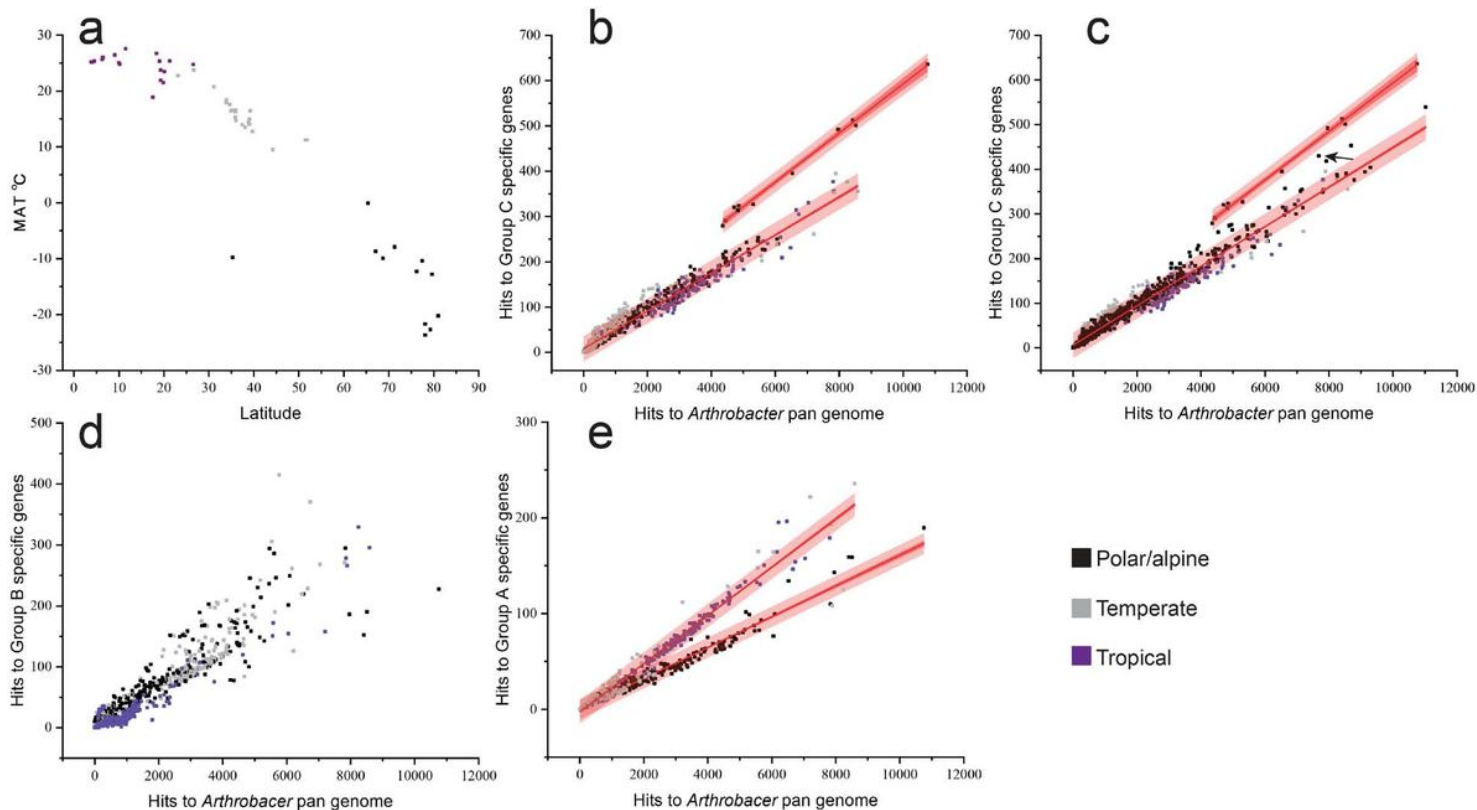


Figure 5

Metagenome analysis of Group C *Arthrobacter*. (a) Depiction of the (mean annual temperature (MAT) of surface air at a height of 2 m (European Centre for Medium-Range Weather Forecasts) relative to latitude. The 797 metagenomes are divided into thermal categories: PA (black squares, 286 metagenome), temperate (grey squares, 294 metagenomes) and tropical (purple squares, 217 metagenomes). (b) Linear regression showing the correlation of the abundance of Group C-specific genes within each of the 797 metagenomes (see panel (a)) relative to the abundance of Group C-specific genes within the *Arthrobacter* pan genome. The 95% prediction interval (dark red band) and 95% confidence interval (light red band) is shown for each regression line (panels b, c and e). The upper cluster contains 11 Axel Heiberg Island permafrost metagenomes. (c) As for panel (b), except with the addition of 361 permafrost metagenomes (total 1158 metagenomes). The Stordalen Mire (Abisko, Sweden) metagenome is shown by an arrow. (d) As for panel (b), except showing Group B-specific genes. (e) As for panel (b), except showing Group A-specific genes present in PA genomes (lower line) and NPA genomes (upper line). The regression line for the 11 Axel Heiberg Island permafrost metagenomes is not shown.

Supplementary Files

This is a list of supplementary files associated with this preprint. Click to download.

- [CavicchioliSupplementaryinformation.pdf](#)
- [CavicchioliTableS1.xlsx](#)

- [CavicchioliTableS2.xlsx](#)
- [CavicchioliTableS3.xlsx](#)
- [CavicchioliTableS4.xlsx](#)
- [CavicchioliTableS5.xlsx](#)
- [CavicchioliTableS6.xlsx](#)
- [CavicchioliTableS8.xlsx](#)